Applied Catalysis B: Environmental 145 (2014) 205–215

Contents lists available at ScienceDirect

Applied Catalysis B: Environmental

journal homepage: www.elsevier.com/locate/apcatb

Catalytic conversion of rapeseed oil for the production of raw chemicals, fuels and carbon nanotubes over Ni-modified nanocrystalline and hierarchical ZSM-5

J.A. Botas[a,*], D.P. Serrano[a,b], A. García[c], R. Ramos[a]

[a] Department of Chemical and Energy Technology, ESCET, Universidad Rey Juan Carlos, c/Tulipán s/n, 28933 Móstoles, Madrid, Spain
[b] IMDEA Energy Institute, Avda. Ramón de la Sagra 3, 28933 Móstoles, Madrid, Spain
[c] Department of Chemical and Environmental Technology, ESCET, Universidad Rey Juan Carlos, c/Tulipán s/n, 28933 Móstoles, Madrid, Spain

ARTICLE INFO

Article history:
Received 22 October 2012
Received in revised form
14 December 2012
Accepted 17 December 2012
Available online 25 December 2012

Keywords:
Rapeseed oil
Nickel
ZSM-5 zeolite
Hierarchical zeolite

ABSTRACT

Catalytic conversion of rapeseed oil has been investigated over nanocrystalline and hierarchical ZSM-5 zeolites aimed to the production of both raw chemicals and fuels. Ni has been added to some of the samples in order to induce bifunctional properties in the catalysts. Almost total rapeseed conversion and deoxygenation degree were achieved with all the catalysts. The main products were gaseous olefins (mostly ethylene and propylene) and aromatic compounds (benzene, toluene and xylenes), which have high interest as raw chemicals. Likewise, high hydrogen contents are found in the gaseous stream since the operating conditions employed (high reaction temperature and atmospheric pressure) favor the occurrence of dehydrogenation reactions. The introduction of hierarchical porosity in ZSM-5 increases the production of light olefins at the expense of aromatic compounds, showing the close relationship between these two types of hydrocarbons. Hierarchical zeolites exhibit enhanced accessibility and diffusion rates, which hinders secondary reactions of the primary cracking products. Ni-containing catalysts show an enhanced dehydrogenation activity as denoted by the increased hydrogen, light olefins and coke production. Important changes were observed in the catalytic activity along time on stream, with a progressive increase in the fraction of aliphatic hydrocarbons. Interestingly, the coke formed over the Ni-containing ZSM-5 samples is in the form of carbon nanotubes, which grow causing a segregation of the Ni particle from the zeolite support. This effect is attenuated in the hierarchical zeolites because the secondary porosity stabilizes the metal particles. In summary, rapeseed oil can be transformed into valuable products (hydrogen, light olefins, aromatic hydrocarbons and carbon nanotubes) by using tailored Ni-containing nanocrystalline and hierarchical ZSM-5 zeolites.

1. Introduction

Oleaginous biomass, such as vegetable oils, has a high interest for the production of biofuels and chemicals that can replace, at least partially, petroleum-derived products [1,2]. Vegetable oils are comprised of triglyceride molecules, which are made up of one mole of glycerol and three moles of fatty acids. Compared to other biomass resources, triglycerides present a relatively high energy density due to their low oxygen content [3]. However, they also possess certain properties, such as high viscosity and low volatility, which prevent their direct use as transportation fuels. Therefore, triglycerides must be processed to yield more valuable fuels and/or raw chemicals.

Among the different routes for the conversion of vegetable oils, transesterification and catalytic cracking have arisen high interest in recent years [4,5]. Transesterification of triglyceride molecules with an alcohol yields biodiesel and glycerin [6,7]. Biodiesel can be blended with petroleum-based fuels in diesel engines. Glycerin also has uses in a variety of industries, but its excessive production, roughly 10% of the feedstock, is becoming this product in a waste problem.

Alternatively, by means of catalytic cracking, vegetable oils can be converted into hydrocarbons in the absence of oxygen at atmospheric pressure and at a relatively low temperature (400 °C–600 °C). The hydrocarbon product distribution so obtained ranges from gaseous compounds to diesel, depending mainly on the operating conditions and the type of catalyst employed [8,9]. Compared to other processes, catalytic cracking presents the advantages of not requiring an external hydrogen source and of leading to products very similar to those obtained from fossil fuels, so they can be directly applied in conventional combustion engines without any adaptation or limitation in the proportion of biofuel content. Moreover, these hydrocarbons can be also used as a feedstock for the petrochemical industry [10,11]. Depending on the features of

* Corresponding author. Tel.: +34 91 488 70 08; fax: +34 91 488 70 68.
E-mail address: juanangel.botas@urjc.es (J.A. Botas).

0926-3373/$ – see front matter © 2012 Elsevier B.V. All rights reserved.
http://dx.doi.org/10.1016/j.apcatb.2012.12.023

the catalyst employed for the conversion of vegetable oils, the selectivity toward different types of products can be adjusted. The development of efficient catalysts, which exhibit a good combination of activity, selectivity and deactivation resistance is essential to optimize the processing of vegetable oils by catalytic cracking. One of the most frequently employed catalysts in the petrochemical industry is ZSM-5 zeolite [12]. This material combines a strong acidity, which promotes the cracking of the feedstock molecules with a remarkable shape-selectivity due to its microporosity. Compared to other zeolites, ZSM-5 also shows a high resistance to deactivation as a consequence of its three dimensional and well-connected micropore system and the ability for cracking coke precursors [13].

In reactions involving bulky molecules, such as triglycerides conversion, catalyst accessibility and textural properties have a strong effect on the overall catalytic performance as the latter may suffer from steric and diffusion limitations. Conventional zeolites, having micrometer crystal sizes, present a low accessibility of bulky molecules to the active sites since most of them are located within the micropores. For that reason, several works have been reported in the last years focused on the conversion of vegetable oils using ordered mesoporous materials [14,15] and hybrid zeolitic ordered mesoporous materials [16,17]. However, despite showing a higher accessibility, these materials exhibit a lower acidity and hydrothermal stability than zeolites. Since the reduction of the crystal size leads to a higher external surface area and decreases the steric and diffusional limitations, nanocrystalline zeolites have been used in the catalytic cracking of vegetable oils [18,19]. Similarly, hierarchical zeolites can be of a high interest for vegetable oils conversion due to their enhanced accessibility as a consequence of the presence of a bimodal porosity, formed by a secondary mesoporosity in addition to the typical zeolitic micropores. The presence of hierarchical porosity in zeolites usually results in a higher catalytic activity for the conversion of large compounds, as it is expected to be the case of triglyceride molecules.

Incorporation of metal active phases to zeolites provides them bi-functional properties showing both acid and metal sites. Thus, the presence of some metals, such as nickel, is expected to promote hydrogenation/dehydrogenation reactions, enhancing the production of high quality hydrocarbons without additional hydrogen consumption [20]. Additionally, the bimodal micro/mesopore size distribution, presented in the hierarchical zeolites, may enhance the dispersion of the nickel species and their interaction with the zeolitic support. Bifunctional zeolitic materials have been employed recently in the catalytic conversion of vegetable oils [21]. The incorporation of molybdenum and nickel into an acidic ZSM-5 support resulted in significant changes in the catalytic performance. These effects were more pronounced in case of Ni/ZSM-5 increasing the production of light olefins at the expense of aromatic hydrocarbons.

In the present work, hierarchical ZSM-5 zeolite samples, with different contribution of the secondary porosity, have been employed for preparing bifunctional catalysts by incorporating Ni particles. The enhanced mesopore surface area and volume present in hierarchical ZSM-5 is expected to increase the accessibility of the reactant molecules and the dispersion of the metal phase, offering new possibilities for tuning the catalytic activity and, more importantly the product distribution, in the conversion of rapeseed oil. The results obtained have shown that, under selected operating conditions, this catalytic system lead to the selective production of a number of compounds that can be used as raw chemicals: hydrogen and light olefins in the gaseous fraction and aromatic hydrocarbons in the liquid products. Moreover, it has been found that coke is deposited over this system mainly in the form of carbon nanotubes, which opens the possibility of preparing a high added-value co-product from vegetable oils.

2. Experimental

2.1. Catalysts preparation

The catalysts used in the present work were prepared using a commercial nanocrystalline ZSM-5 zeolite (Si/Al = 36), also used as reference catalyst, provided by SÜD-CHEMIE and hierarchical h-ZSM-5 zeolites (Si/Al = 30) synthesized according to a procedure previously developed by our research group [22]. This method is based on the use of a silanization agent to prevent the total aggregation of protozeolitic nanounits during the crystallization step, leading to zeolitic materials containing a hierarchical porosity. This strategy was applied in the present work to the synthesis of the hierarchical ZSM-5 zeolite, using phenylaminopropyl-trimethoxysilane (PHAPTMS) as the silanization agent, tetrapropylammonium hydroxide (TPAOH) as the zeolite structure-directing agent and aluminum isopropoxide (AIP) and tetraethylorthosilicate (TEOS) as aluminum and silica sources, respectively. Following this method, different samples were prepared by adding PHAPTMS in different proportions (5, 8 and 12 wt.%) with respect to the total silica content in the synthesis gel.

The hierarchical zeolite with the highest proportion of PHAPTMS (12 wt.%) and the commercial nanocrystalline zeolite were also modified by the incorporation of nickel (metal loading 6–7 wt.%). The metal addition was carried out by wetness-impregnation, using as precursor hexahydrate nickel nitrate. Firstly, the parent zeolites were outgassed at room temperature under vacuum for 1 h. After that, a solution with the proper concentration of the precursor was added to the samples. In order to distribute homogeneously the added solution into the solid internal structure and evaporate the solvent for metal precursor incorporation, impregnated samples were introduced in a rotary evaporator under vacuum at 60 °C for 60 min. Subsequently, the dried samples were calcined in air at 550 °C for 5 h (heating rate 1.8 °C min^{-1}). Finally, a reduction treatment was performed under pure hydrogen flow (20 cm^3 min^{-1}) at 550 °C for 2 h (heating rate 10 °C min^{-1}).

2.2. Catalysts characterization

The prepared catalysts were characterized by means of conventional techniques to determine their physicochemical properties. X-ray diffraction was performed in a Philips X'PERT MPD diffractometer using Cu-Kα radiation. XRD diffractograms were recorded within the 5–50° range using a step size of 0.1° and a counting time of 10 s. The Si/Al atomic ratio of all the resulting catalysts and the total amount of nickel of the impregnated samples were determined by inductively coupled plasma atomic emission spectroscopy (ICP-AES) using a Varian VISTA-AX CCD spectrophotometer. The textural properties were determined from the argon adsorption isotherms at 87 K, which were obtained using a Quantachrome AUTOSORB instrument. Previously, the samples were outgassed at 300 °C for 3 h under vacuum ($P < 10^{-5}$ mmHg). The overall surface area was calculated applying the BET equation, whereas the contribution of the secondary mesoporosity, in terms of both surface are and micropore volume, were determined by the non local density functional theory (NLDFT) [23] model assuming cylindrical pore geometry.

The acid properties were measured by ammonia temperature programmed desorption (TPD) in a Micrometrics 2910 equipment using helium as carrier gas. Prior to ammonia desorption, the samples were outgassed under helium flow (50 cm^3 min^{-1}), using a heating rate of 15 °C min^{-1} up to 550 °C and remaining at this temperature for 30 min. Then, the sample was cooled and saturated under ammonia flow (35 cm^3 min^{-1}) for 30 min at 180 °C. Subsequently, the physisorbed ammonia was removed

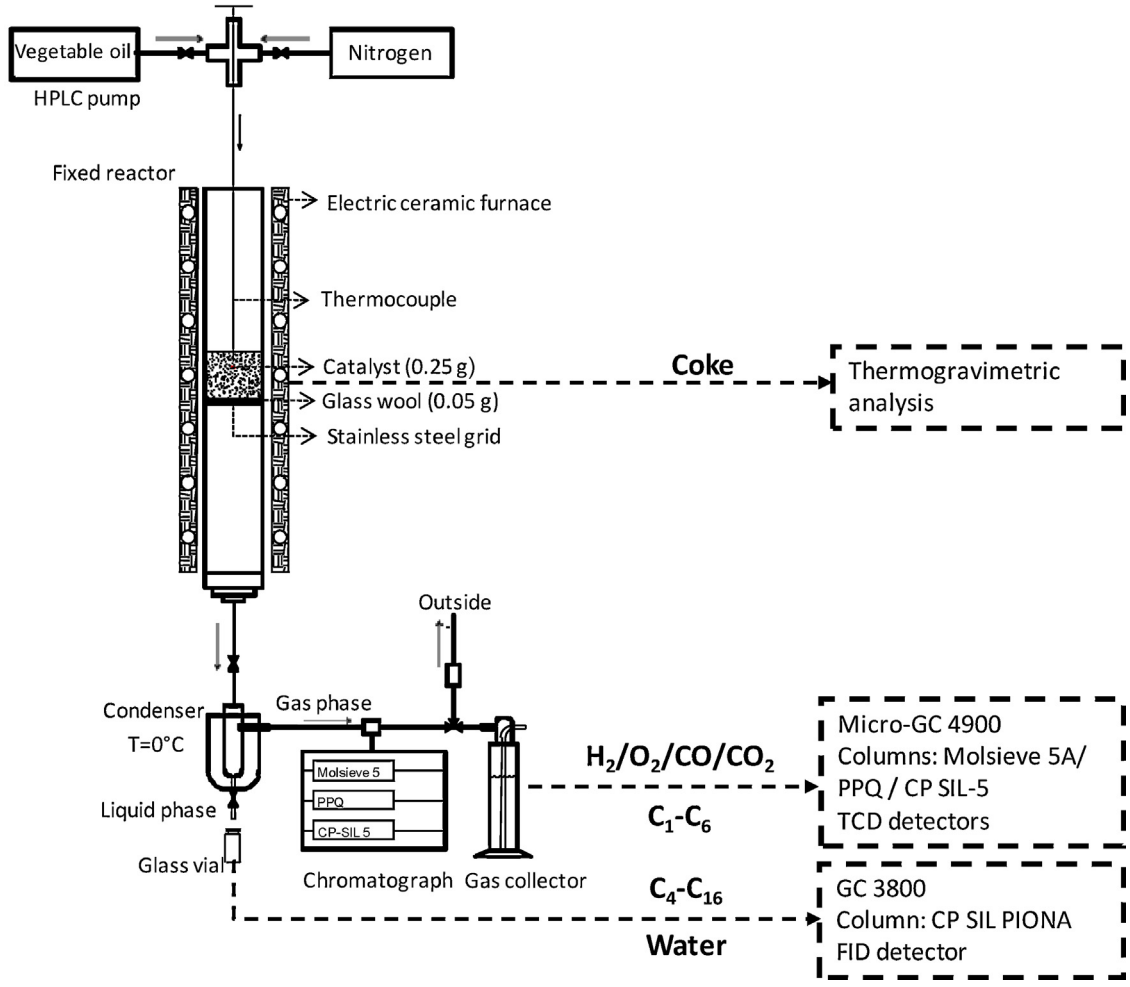

Fig. 1. Schematic diagram of the experimental installation and method for the collection and analysis of the products from the catalytic conversion of rapeseed oil.

by flowing He (50 $cm^3\,min^{-1}$) at 180 °C for 90 min. Finally, the chemically adsorbed ammonia was desorbed by increasing the temperature up to 550 °C with a heating rate of 15 °C min^{-1} in flowing He (50 $cm^3\,min^{-1}$). By means of a thermal conductivity detector (TCD), the ammonia concentration in the helium stream was recorded continuously.

TEM images of the fresh and used catalysts were obtained by transmission electron microscopy (TEM) using a PHILIPS TECNAI 20 electron microscopy operating at 200 kV. Previously, the analyzed samples were dispersed in acetone solution, stirred in an ultrasonic bath and deposited on a carbon-coated Cu grid. Thermogravimetric analyses of the used catalysts were carried out to determine the amount of coke deposited over the catalyst. They were performed under flowing air (100 $cm^3\,min^{-1}$) on a SDT 2960 Simultaneous DSC-TGA thermogravimetric analyzer (detection limit 0.04 μg). Samples were loaded on a platinum microcrucible and heated at 10 °C min^{-1} up to 1000 °C, recording continuously the weight of each sample.

2.3. Catalytic experiments

The performance of the catalysts for rapeseed oil conversions was studied in a fixed-bed down flow reactor (stainless steel, 10 mm internal diameter and 300 mm length) at atmospheric pressure under nitrogen. The rapeseed oil was obtained from *Gustav Heess* and was of the degummed and refined variety. Details concerning the physicochemical properties of rapeseed oil are given elsewhere [21].

Fig. 1 shows a scheme of the experimental setup used for the present work. The catalyst (0.25 g each run) was set over a thin coat of glass wool supported in a stainless steel grid positioned centrally within the reactor. The feeding of rapeseed oil was carried out by means of a HPLC pump (operability 0.01–5 $cm^3\,min^{-1}$). The reactor was previously heated up to the desired temperature (550 °C) under nitrogen flow by an electric ceramic furnace whose temperature was controlled by a thermocouple placed inside the catalyst bed.

Once the operating temperature was reached, the nitrogen flow was stopped and rapeseed oil was fed into the reactor at the predetermined space velocity (7.6 h^{-1}), being the oil conversion complete under these conditions [21]. A time of 30 min was allowed for reaching steady flow conditions. Thereafter, the samples were collected for periods of 60 min, during a total reaction time of 180 min. The product mixture leaving the reactor was separated into gaseous and liquid phases employing a condenser at 0 °C. The gaseous fraction was directed toward a glass water trap, whereas the liquid products remained in the condenser. After collecting the last sample, the feeding of the oil was stopped and the reactor was left cooling down to room temperature. Finally, the catalyst, previously washed with acetone and dried inside the reactor, was recovered to study the formation of solid deposits of coke.

The gaseous products were analyzed using a VARIAN micro-GC-CP4900 chromatograph, equipped with three chromatographic columns (5A Molsieve, PPQ, CP-SIL 5) and provided with separate

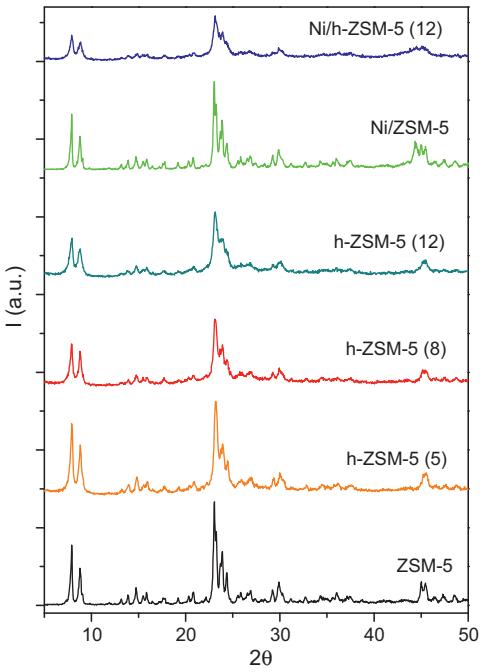

Fig. 2. XRD patterns of the ZSM-5 catalysts.

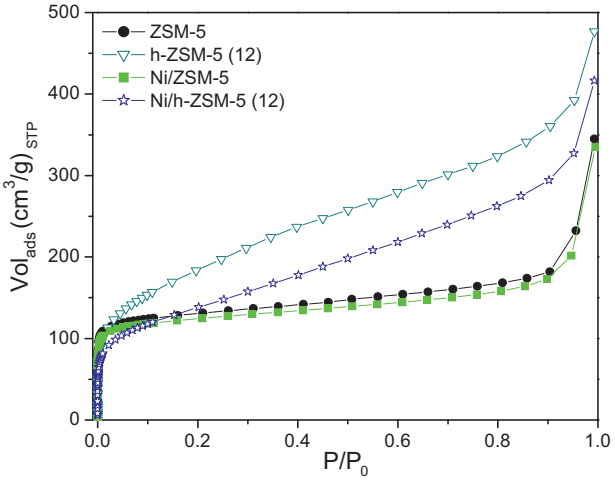

Fig. 3. Ar adsorption isotherms at 87 K of the ZSM-5 catalysts.

injectors and detectors (TCD). In the first column, Ar was employed as carrier gas whereas in PPQ and CP-SIL 5 columns the used carrier gas was He. These 3 columns were previously calibrated to detect and quantify gaseous compounds such as H_2, O_2, N_2, CO, CO_2, and hydrocarbons from C_1 to C_6. The liquid fraction was composed by an organic phase and water. The water phase was removed by decantation and weighted. The liquid organic products were analyzed with a VARIAN GC-3800 chromatograph equipped with a column CP SIL PIONA (0.25 mm internal diameter and 100 m length) and a flame ionization detector (FID). This equipment allows indentifying and quantifying hydrocarbons in the range C_4–C_{16}. The amount and type of coke formed were determined by thermogravimetric studies of the used catalysts.

3. Results and discussion

3.1. Catalysts properties

The catalysts have been characterized by a number of standard techniques in order to determine their physicochemical properties. XRD diffractograms of the samples are shown in Fig. 2. The XRD patterns are coincident with that of the MFI zeolitic structure, although for the hierarchical samples the X-ray diffraction peaks are less intense as the amount of PHAPTMS is increased. There is also a broadening of the reflections compared to the commercial nanocrystalline ZSM-5. This effect confirms that the hierarchical zeolite samples present smaller crystalline domains [24]. The addition of Ni does not affect the crystallinity of these materials.

The results of ICP-AES analysis of studied materials are included in Table 1. All the samples show comparable Si/Al atomic ratios. In the case of the synthesized ZSM-5 samples this ratio is very close to that of the starting gel, indicating that both Si and Al species are incorporated in similar proportions to the zeolite structure. In the case of the impregnated catalysts both materials present also a comparable Ni content, although slightly lower than the theoretical value (7 wt.%).

Fig. 3 illustrates the Ar adsorption isotherms measured at 87 K. All the materials show a high Ar adsorption at low relative pressures, which corresponds with micropore filling. However, in the case of the hierarchical zeolites the isotherms exhibit an enhanced Ar adsorption at intermediate relative pressures ($0.2 < P/P_0 < 0.9$), due to the argon adsorption on both mesopores and external surface [25]. These results confirm that the hierarchical samples show a secondary porosity originated by the presence of mesopores between the zeolite nanounits. When Ni is incorporated to the zeolitic support, a reduction of the Ar adsorption takes place. This effect is more pronounced in the case of the hierarchical ZSM-5 sample, indicating that a great part of the Ni particles are deposited inside the secondary porosity.

Based on the analysis of the experimental data from Ar adsorption isotherms the textural properties of the resulting catalysts have been determined (see Table 1). Thus, the specific surface area was calculated by the BET method, whereas the external and microporous surfaces were estimated using the NLDFT model. These results show an enhanced BET and external/mesopore surface areas for the hierarchical zeolites. The mesopore surface areas of these materials are especially high representing about 55–63% of the total surface area (BET). In the case of nanocrystalline ZSM-5 this value is around 19% of the total surface area. The enhancement of the textural properties increases with the amount of silanization agent added to the synthesis gel, reaching a maximum value for the sample prepared with 12 wt.% of PHAPTMS ($S_{BET} = 586\ m^2\ g^{-1}$ and $S_{ext} = 373\ m^2\ g^{-1}$). On the other hand, the micropore surface and volume show the opposite trend. These changes in the textural properties are expected to have a positive effect on the accessibility to the active sites and, therefore, on the catalytic activity for the conversion of bulky molecules. The addition of Ni to the nanocrystalline ZSM-5 sample causes just a small decrease in the value of the textural properties. However, for the hierarchical h-ZSM-5 (12) sample a strong reduction is observed in the surface area and pore volume values. Thus, micropore surface area decreases by 19%, whereas the external/mesopore surface area undergoes a 29% reduction, after the Ni incorporation. These results suggest that a great part of the Ni particles are located on the secondary porosity of hierarchical ZSM-5.

Representative TEM images of fresh catalysts are shown in Fig. 4. The commercial ZSM-5 zeolite presents nanosized crystals in the range 20–80 nm. However, the images corresponding to the hierarchical zeolites show aggregates with a size around 200 nm, formed by quite smaller nanounits (10–20 nm). TEM micrographs of the impregnated catalysts show the presence of rounded Ni particles (10–50 nm). In the case of the nanocrystalline ZSM-5, the Ni particles are located mostly on the edges and external surface of the crystals. However, in case of the hierarchical zeolite (h-ZSM-5 (12)),

Table 1
Physicochemical properties of the ZSM-5 catalysts.

Catalyst	Si/Al[a]	Metal content[a] (wt.%)	S_{BET} [b] ($m^2\ g^{-1}$)	$S_{ext/mes}$ [b] ($m^2\ g^{-1}$)	S_{mic} [b] ($m^2\ g^{-1}$)	Micropore[b] volume ($cm^3\ g^{-1}$)	Acid sites[c] (mequiv. $NH_3\ g^{-1}$)	T_{max} [d] (°C)
ZSM-5	36	–	404	77	327	0.207	0.424	365
h-ZSM-5 (5)	31	–	535	294	240	0.152	0.355	338
h-ZSM-5 (8)	30	–	561	345	215	0.136	0.318	348
h-ZSM-5 (12)	30	–	586	373	212	0.134	0.308	332
Ni/ZSM-5	36	6.25	385	67	318	0.201	0.106/0.295	308/365
Ni/h-ZSM-5 (12)	30	6.98	436	266	170	0.107	0.050/0.325	275/350

[a] ICP-AES measurements.
[b] Argon adsorption at 87 K.
[c] Ammonia TPD experiments.
[d] Temperature maxima of the peak as determined by TPD-NH_3 experiments.

Ni particles are perceptible within the secondary porosity created by the aggregation of nanocrystal units, causing a better dispersion and a stronger interaction of the metal active phase with the zeolitic support [26].

The acid properties of the samples, measured by ammonia TPD, are summarized in Table 1. The commercial nanocrystalline zeolite ZSM-5 exhibits the highest amount of acid sites (0.424 mequiv. $NH_3\ g^{-1}$). This value decreases in the series of hierarchical zeolites up to 0.308 mequiv. $NH_3\ g^{-1}$ for the sample prepared with a 12 wt.% of PHAPTMS. Since the aluminum content is quite similar, this decrease in the acidity may be related to the presence of weaker acid centers in the hierarchical zeolites, which desorb ammonia at the starting temperature (180 °C) during the purge step before the TPD. As it has been reported in the literature [27], the acid sites located on the external/mesopore surface have a lower acid strength than those inside the micropore system. In consequence, some of these acid sites are not detected in the TPD experiment. Differences in the values of the maximum temperature of ammonia desorption may be explained by this loss of acid strength, although they may be also related to differences

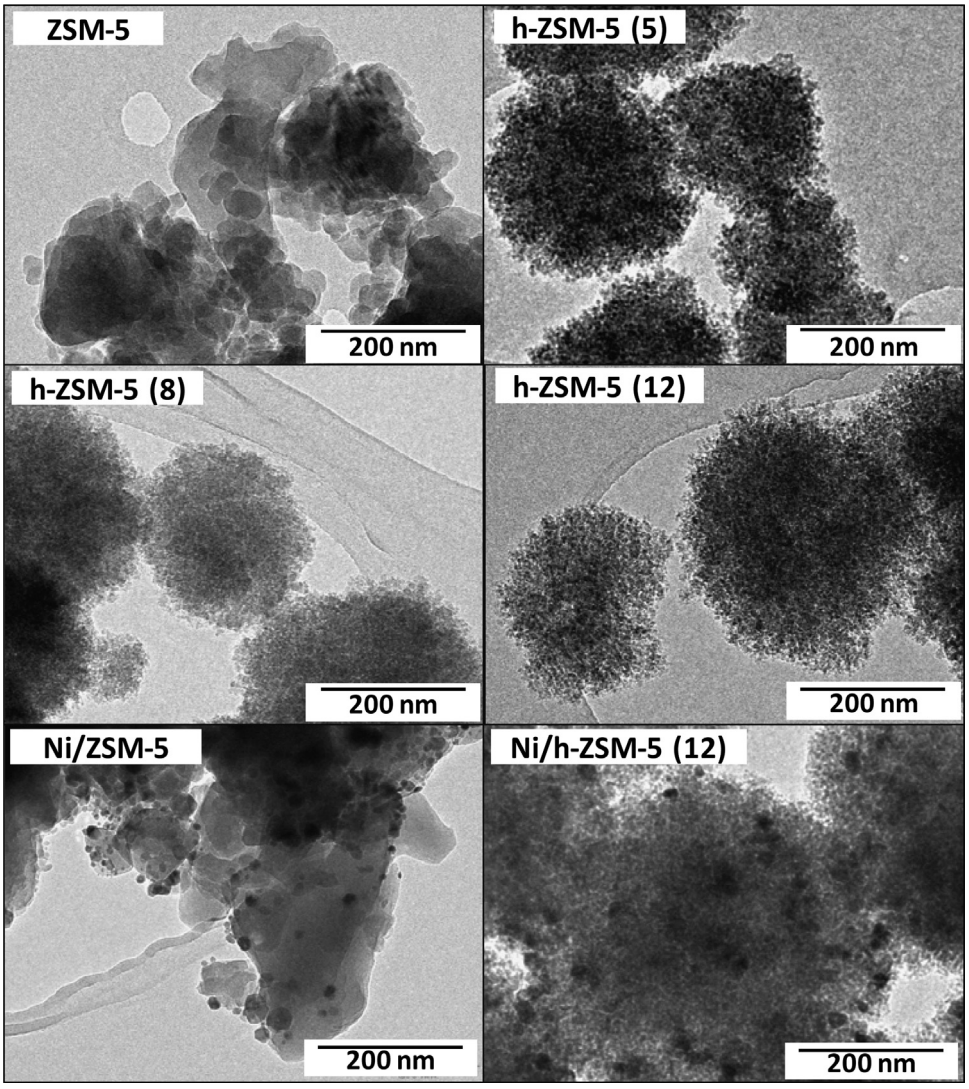

Fig. 4. TEM images of fresh catalysts.

in the zeolite crystal sizes. The really small size of the nanounits in hierarchical zeolites is expected to lead to minor diffusional restrictions for ammonia diffusion than larger ones. Regarding the incorporation of Ni, it appears to affect both the amount and the maximum temperature of ammonia desorption, probably due to the formation of new acid sites. Thus, a small temperature peak (maximum at about 308 °C) is clearly observed for the Ni/ZSM-5 sample, being probably originated by Ni species with weak acidic features. In the case of the hierarchical Ni/h-ZSM-5 (12) sample, this low-temperature peak is also observed but with a smaller contribution, whereas the second peak becomes broader and shifted toward higher temperatures compared to the Ni-free hierarchical ZSM-5. These results can be interpreted by the better dispersion and contact of the Ni particles with the zeolitic support in the case of the hierarchical zeolite samples, as observed in the TEM images.

3.2. Catalytic conversion of rapeseed oil

The synthesized catalysts were studied for rapeseed oil conversion. All the tests were carried out with a reaction time of 180 min, taking samples accumulated for periods of 60 min, at temperature of 550 °C and using a weight hour space velocity of 7.64 h^{-1}. An inert atmosphere (nitrogen) was employed and no external hydrogen source was added. The selection of these operation conditions was made attending to previous results [21].

In a preliminary blank experiment, carried out using an empty reactor, it was obtained an almost total conversion of the rapeseed oil. This implies that the reactant is thermally converted, which can be assigned to the high reaction temperature employed (550 °C). Compared with the catalytic reactions, in the absence of catalyst the production of gases was considerably lower, whereas an increase in the liquid phase yield takes place (close to 95 wt.% referred to the total of products). A high proportion of unknown products were obtained in the liquid fraction (C_{11+}) of the blank experiment, likely due to the formation of oxygenated compounds such as acids, alcohols, ketones, etc. Moreover, water was not detected between the thermal degradation products and the formation of CO and CO_2 was significantly lower (the gas phase was mainly formed by carbon monoxide), indicating that some deoxygenation via decarbonylation occurs even in the absence of catalysts, although in a less effective way compared to the catalytic tests. Likewise, the products obtained in the thermal degradation contain a little proportion of light olefins and aromatic hydrocarbons, which are the target pursued in this work.

Fig. 5 shows the overall product distribution obtained with the different tested catalysts. The oxygen content present in the feedstock (8.9 wt.%) resulted in the formation of light oxygenated compounds such as carbon monoxide, carbon dioxide and water, with a practically total deoxygenation degree. It is generally assumed that they are produced by deoxygenation reactions of heavy oxygenated species coming from thermal decomposition of the feedstock [11]. Since no other oxygenated compounds (like ketones, alcohols, acids, etc.) have been detected, it appears that the main routes for deoxygenation are decarbonylation, decarboxylation and dehydration. Significant changes are observed in the relative contribution of these paths for the removal of oxygen when Ni was added. Thus, impregnated Ni samples enhanced the formation of carbon dioxide, whereas the production of water was reduced. This effect suggests that the presence of Ni favors the deoxygenation via decarboxylation.

As a consequence of the deoxygenation reactions, relatively heavy hydrocarbons are formed which subsequently undergo different reactions to yield a wide range of hydrocarbons (between 80 and 86 wt.% yield) from gaseous to diesel hydrocarbons. As it is shown in Fig. 5, a high production of gaseous (>37 wt.%) and gasoline (>32 wt.%) hydrocarbon fractions was obtained compared

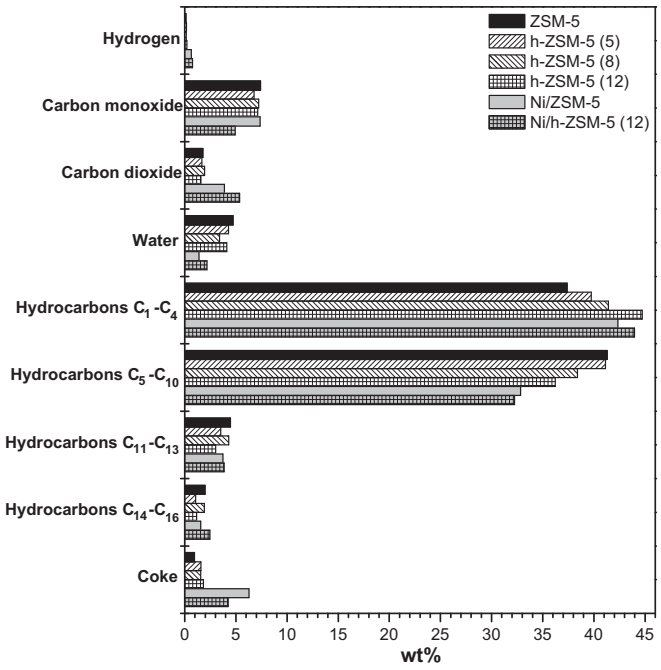

Fig. 5. Conversion of rapeseed oil over the ZSM-5 catalysts: 0–180 min overall product distribution.

to kerosene (<4.5 wt.%) and diesel (<2.5 wt.%). Hydrocarbons with carbon atom numbers higher than 16 were not detected, which indicates that a complete conversion of the original triglycerides and of the corresponding C_{18} fatty acids has taken place. The formation of a high proportion of gaseous hydrocarbons agrees well with the strong acidity and small pore size present in the ZSM-5 zeolite, which promote extensive cracking reactions. It should be taken into account that cracking reactions usually take place through the formation of carbenium ions over strong acid sites. Both, the incorporation of nickel, as well as the presence of the secondary porosity in the hierarchical zeolites, increased the formation of C_1–C_4 hydrocarbons at expense of those within the gasoline range. The hierarchical porosity increases the cracking activity and avoids secondary reactions of the primary products, despite the lower and weaker acidity of the hierarchical ZSM-5 samples, due to the reduction of steric and internal diffusion hindrances.

The incorporation of Ni also promotes the formation of gaseous hydrocarbons likely associated to the occurrence of hydrogen transfer reactions, which increase the formation of light olefins. The role played by the Ni species as promoter of hydrogenation/dehydrogenation is also responsible of the increase in the hydrogen formation, as observed in Fig. 6 showing the composition of the gaseous phase in terms of mole percentage. For the purely acidic ZSM-5 samples, the hydrogen present in the gases is about 4–5 wt.%, whereas it is sharply increased for the Ni-containing catalysts. Simultaneously, as it can be observed in Fig. 5, the incorporation of Ni also enhances sharply the coke deposited over the catalyst. These results show that Ni particles promote dehydrogenation reactions in a great extension. This is probably favored by the conditions employed in the catalytic tests: absence of external hydrogen sources, relatively high reaction temperatures and operation at atmospheric pressure. Moreover, the dehydrogenation role of the Ni species is even more pronounced for the hierarchical ZSM-5 samples, as denoted by the high hydrogen concentration (about 20 mol%) present in the gases obtained over the Ni/h-ZSM-5 (12) catalyst. This synergetic effect between Ni incorporation and hierarchical porosity can be explained by the improved dispersion and

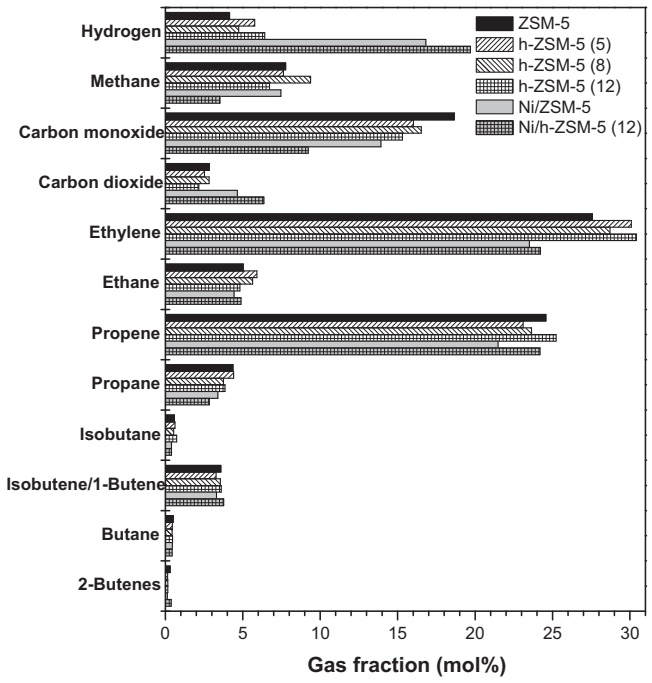

Fig. 6. Conversion of rapeseed oil over the ZSM-5 catalysts: 0–180 min total gas composition.

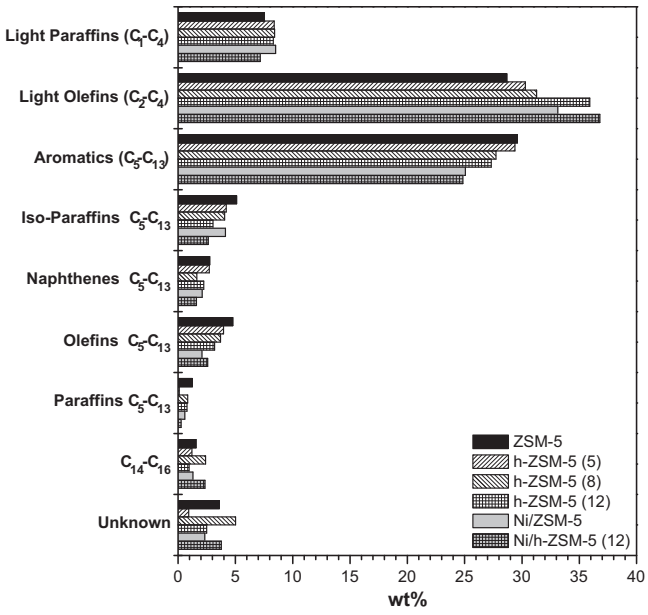

Fig. 7. Conversion of rapeseed oil over the ZSM-5 catalysts: 0–180 min product distribution by hydrocarbon groups.

contact of the metal particles over the zeolitic supports of these samples, as above denoted.

The hydrogen contained in the gas stream increases its heating value. Alternatively, this hydrogen could be separated for being commercially applied. In addition to hydrogen, the gaseous fractions contain other interesting compounds regarding their possible use as raw chemicals. This is the case of the different light olefins present in significant concentrations: ethylene, propylene, and butenes. Considered together, just ethylene and propene account for more than 50 mol% of the produced gases. Other hydrocarbons identified in the gaseous stream include methane, ethane and butanes, which could be used as a heat source for providing most of the energy inputs required in the process.

The product distribution, according to hydrocarbon fractions and types, obtained in the rapeseed oil catalytic conversion, is illustrated in Fig. 7. This distribution shows a high selectivity for light olefins and aromatic hydrocarbons, which are valuable compounds in the petrochemical industry. As indicated above, the light olefins fraction is formed mainly by ethylene and propylene, whereas benzene, toluene and xylenes are the predominant components of the aromatic hydrocarbons. These two fractions are closely connected as the aromatic hydrocarbons are mainly formed by the oligomerization and cyclization of light olefins [11,28,29]. Therefore, as it is displayed in Fig. 7, the production of these two compounds shows usually opposite trends. Similar behaviors, regarding light olefins and aromatic hydrocarbons, have been reported in the literature in catalytic conversion of different feedstocks over ZSM-5 catalysts [30]. Although present in smaller proportions, other types of hydrocarbons, such as linear paraffins, iso-paraffins, naphthenes and C_5–C_{13} olefins, were also produced as a result of a variety of reactions catalyzed by acid and/or metal sites (isomerization, oligomerization, cyclization, etc.). However, significant changes are not appreciated among these fractions with the tested catalysts. It appears that the modifications carried out in the prepared samples do not have large effects on the reaction pathways of these processes. By contrast, it seems that the yield of the two main products, light olefins and aromatic hydrocarbons may be modified by the variation of the physicochemical properties of ZSM-5 catalysts.

The yield of light olefins increased over the hierarchical zeolites, achieving its highest value (36.8 wt.%) for the sample having the maximum proportion of secondary porosity (h-ZSM-5 (12)). This trend is accompanied by a parallel decrease in the amount of aromatic hydrocarbons. The weaker acidity and faster diffusion exhibited by the hierarchical ZSM-5 may explain this behavior. Based on previous works [29,31], light olefins can be considered as primary products from end-cracking reactions of heavier compounds, being subsequently converted into other types of hydrocarbons, mainly aromatics, due to their high reactivity. These secondary reactions take place to a lesser extent over the hierarchical ZSM-5 samples due to the weaker acidity of the sites located on the external/mesopore surface and the faster diffusion through the secondary mesoporosity of the primary oil cracking products. Likewise, the impregnation of the nanocrystalline ZSM-5 and the hierarchical h-ZSM-5 (12) zeolites with nickel increases the production of light olefins, reducing the yield of aromatic hydrocarbons. In this case, the role of nickel generating new active sites, that promote hydrogen transfer reaction, in combination with the reduction of the micropore volume by partial blockage of the micropores, affects also negatively to the conversion of light olefins into aromatics.

The conversion of polyolefins over ZSM-5 and other solid acid catalysts has been extensively reported in previous works of our group [32,33]. Taking into account the similarities existing between polyolefins and vegetable oils cracking, the reaction scheme proposed for polyolefin cracking has been here adapted to describe the major routes for the formation of hydrocarbons in the conversion of vegetable oils using zeolite catalysts (Fig. 8). Firstly, since vegetable oils are thermally unstable, triglycerides are decomposed and undergo deoxygenation reactions, releasing CO, CO_2 and H_2O, to yield relatively heavy hydrocarbons. The length of these hydrocarbon chains is strongly dependent on the initial fatty acid and the operation conditions (temperature, pressure, space velocity, type of reactor, etc.), as well as on the properties of the catalyst employed. In the case of ZSM-5 zeolite, the strong acidity of the catalyst favors end-chain cracking reactions that lead to the formation of light olefins and hydrocarbons with carbon atom numbers within the kerosene–diesel range. Further end-chain cracking of the latter yields both additional light olefins and lighter aliphatic

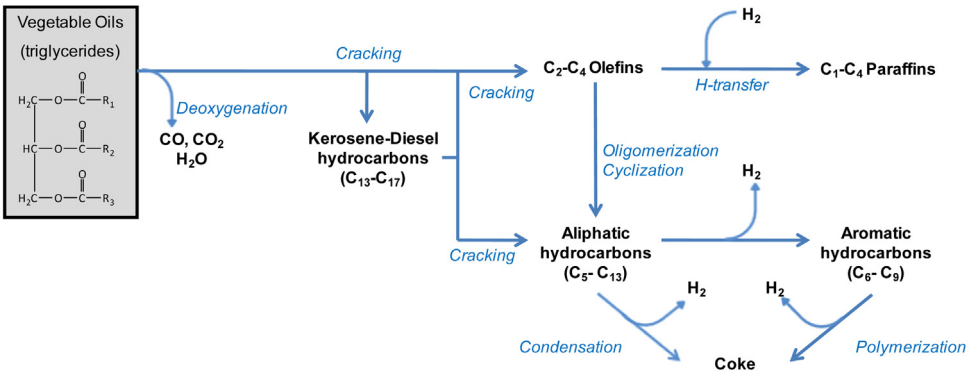

Fig. 8. Proposed reaction pathway for the conversion of vegetable oils over ZSM-5 zeolite.

hydrocarbons belonging mainly to the gasoline boiling point range. These pathways explain the high share of gaseous olefins observed in the product distribution. However, due to their high reactivity, these olefins participate also as reactants in a number of reactions. Thus, by means of hydrogen transfer reactions light olefins are converted into the corresponding light paraffins. Moreover, naphthenic hydrocarbons may be formed by oligomerization and cyclization of light olefins. Likewise, cyclization followed by dehydrogenation eventually tends to produce aromatic hydrocarbons. ZSM-5 zeolite is known to be a catalyst that strongly promotes aromatization reactions, which in this work are also reinforced by the conditions employed: absence of external hydrogen sources and relatively high temperatures. These facts explain the high amounts of aromatics observed in the products coming from rapeseed oil cracking. Finally, aromatic hydrocarbons may undergo polymerization reactions to produce coke, which may be also formed due to the condensation of heavy products over the catalyst surface.

3.3. Evolution of the product distribution along the time on stream

It is known that deactivation by coke formation and deposition over the catalyst is one of the main drawbacks associated to biofuels production by biomass thermochemical processing. Therefore, in order to investigate the influence of the coke deposition over the catalytic activity, the evolution of the product distribution along the time on stream is represented in Fig. 9 for the different catalysts here investigated.

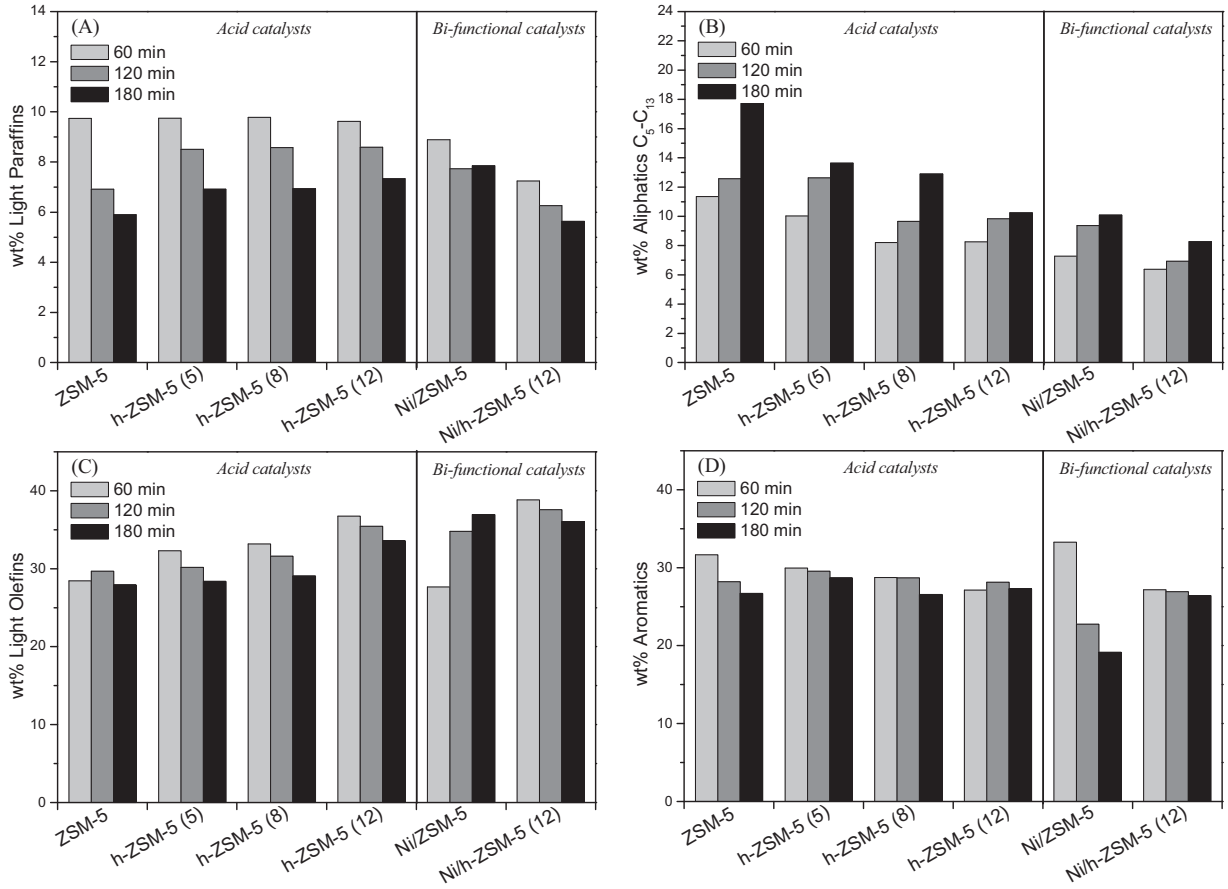

Fig. 9. Conversion of rapeseed oil over the ZSM-5 catalysts: evolution of the product yield with the time on stream.

A common general trend for all the purely acidic catalysts along the time on stream is observed, consisting on the progressive increase in the proportion of aliphatic hydrocarbons (Fig. 9b) at the expense of the rest of the hydrocarbon fractions. Thus, as shown in Fig. 9a and c, the yields in both light paraffins and olefins decreases sharply along the time on stream, whereas aromatic hydrocarbons (Fig. 9d) are affected to a lesser extent. These results are a consequence of the loss of cracking activity due to the progressive formation of coke. The initial long chain hydrocarbons, derived from the deoxygenation of triglycerides, undergo cracking reactions to give a wide range of hydrocarbons. Catalyst deactivation affects negatively to these cracking reactions, inhibiting the conversion of aliphatic hydrocarbons and resulting in a reduction of both light olefins and paraffins.

In the case of the Ni-containing zeolites, the behavior is not the same for the two samples. The hierarchical Ni/h-ZSM-5 (12) exhibits trends in the evolution of the product distribution along the time on stream very similar to those of the above commented for the purely acidic catalysts. However, the Ni-containing nanocrystalline ZSM-5 behaves in a quite different way. While for this sample there is also an increase in the yield of aliphatic hydrocarbons and the paraffins fraction undergo a progressive reduction, an anomalous behavior is observed in the variations observed for light olefins and aromatic hydrocarbons. With this catalyst, a sharp decrease occurs in the production of aromatic compounds, whereas the yield in light olefins is enhanced along the time on stream. These results evidence that the Ni-ZSM-5 catalyst has largely lost along the time on stream the ability for catalyzing the aromatization of light olefins due to the changes suffered by the catalyst phases, as it will be described in a subsequent section of this work.

3.4. Characterization of the deposited coke

The production of coke is the result of the formation of heavy compounds, which are deposited on the catalyst surface causing changes in its catalytic activity. These compounds are not desorbed from the catalyst due to their low volatility or because they are trapped in interior cavities. The main consequence of their formation and deposition is the catalyst deactivation by covering active sites or by blocking the access of reactant molecules to active sites. Regarding this aspect, it is essential the use of characterization techniques in order to determine the nature and location of the formed coke.

The amount of coke deposited over each sample was determined by thermogravimetric analyses (TG) in air. Fig. 10a illustrates the weight loss experimented by each sample, referred to the used catalyst weight. The commercial nanocrystalline ZSM-5 zeolite presents the lowest coke content (~22 wt.%, referred to the fresh catalyst weight). The hierarchical zeolites showed a higher amount of coke (~43 wt.%, referred to the fresh catalyst weight), with no significant differences among them. These values are quite much higher than the maximum amount that could be accumulated inside the ZSM-5 zeolite micropores (around 11 –12 wt.% for a standard ZSM-5 sample), so it is evident that a great part of this coke is deposited over the external surface and the secondary porosity of the nanocrystalline and hierarchical ZSM-5 samples, respectively. On the other hand, the incorporation of Ni to the catalyst causes a further and significant enhancement in the quantity of coke formed. This fact it is in agreement with the reported promotion of coke formation by nickel-modified zeolites [34]. Moreover, these findings are in line with the above commented increase of the hydrogen concentration in the gaseous stream. Under the conditions employed in this work (relatively high temperature and atmospheric pressure), the presence of Ni in the catalyst promotes strongly the extension of dehydrogenation reactions, which result in the formation of high amounts of coke

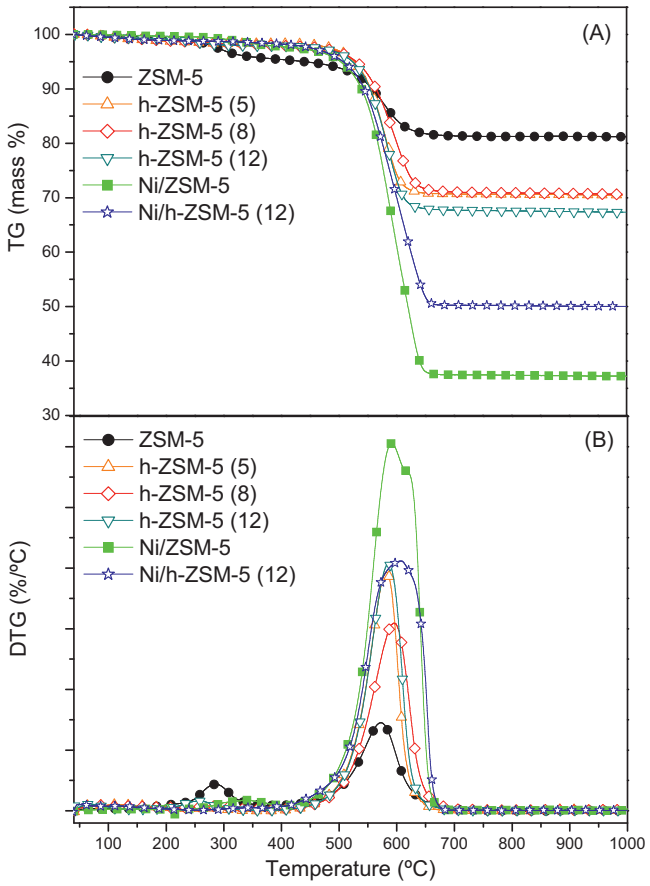

Fig. 10. Thermogravimetric analysis of the spent ZSM-5 catalysts: (a) weight loss as function of temperature (TG), (b) derivative weight loss as function of temperature (DTG).

and the production of hydrogen. Interestingly, in spite of the great amount of coke deposited, the catalyst keeps a significant catalytic activity along the time on stream, which indicates that a great part of the active sites remain still accessible for the reactant molecules.

The derivative of the TG weight loss as function of temperature is displayed in Fig. 10b. The maximum weight loss occurred at around 580 °C for all the tested catalysts, which indicates that most of the deposited coke presents an ordered polyaromatic nature [35]. According to the proposed reaction mechanism, this coke derives mainly from the polymerization/condensation of aromatic hydrocarbons. This is consistent with the decrease in the yield of aromatic hydrocarbons as the reaction progresses. In the case of the nickel-impregnated catalysts, a broadening of this peak is observed indicating a higher contribution from a diversity of compounds. Likewise, a minor peak at 290 °C is denoted for the nanocrystalline ZSM-5, which may correspond with the combustion of heavy hydrocarbons condensed on the external surface of the zeolite crystals [35,36].

TEM images of the used catalysts are shown in Fig. 11, revealing major differences about the morphology and nature of the coke formed on the catalysts. In the case of Ni-free samples coke appears deposited in close contact with the zeolitic support for both nanocrystalline and hierarchical zeolites, so it is not easy to distinguish the features of the carbonaceous deposits. However, for the Ni-containing samples coke is mainly in the form of carbon nanotubes, which growth linked to the Ni particles. Most of these nanotubes are separated from the zeolite crystals, which explains why these catalysts keep a significant catalytic activity even after huge amounts of coke have been formed. Moreover, these TEM

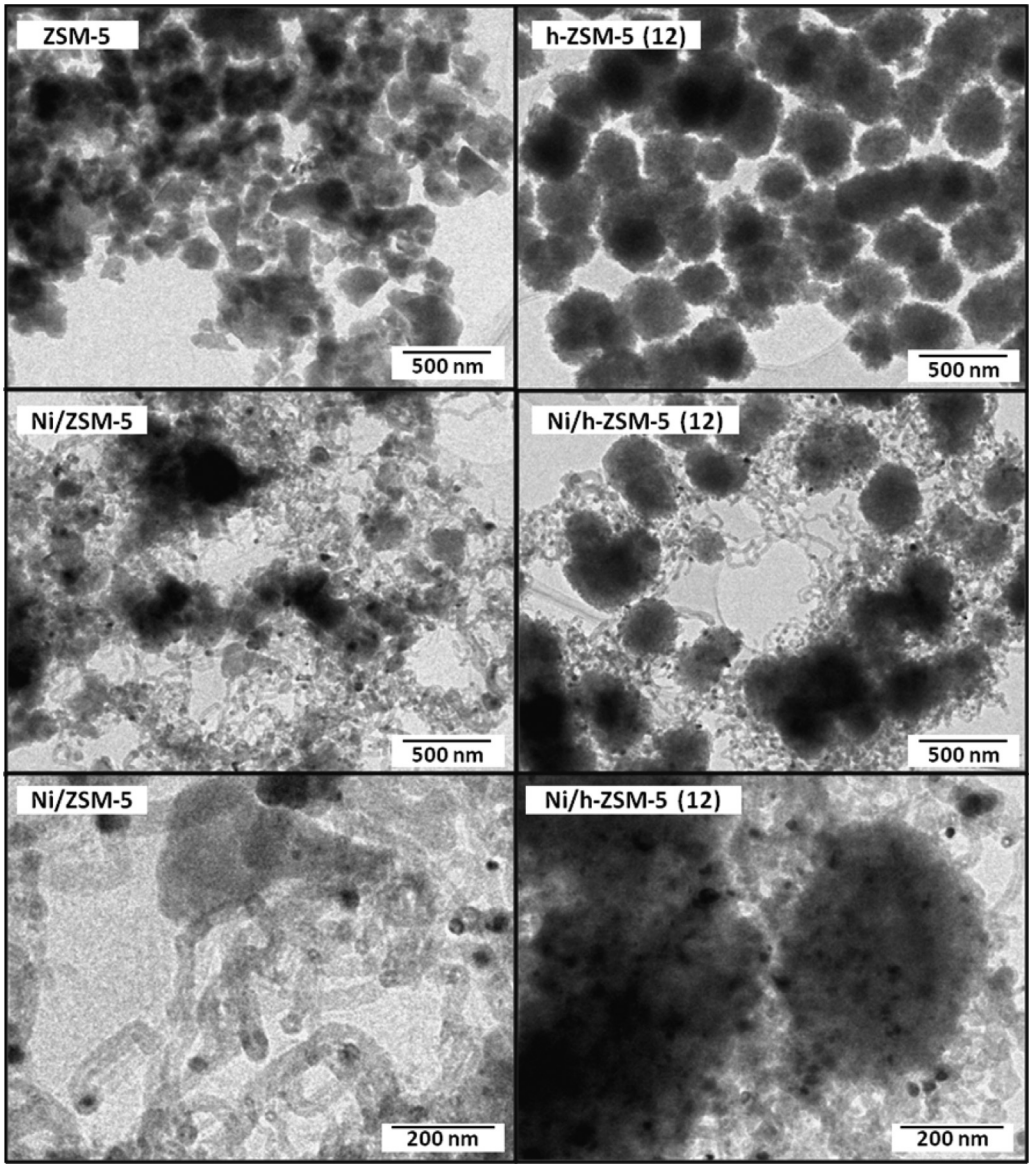

Fig. 11. TEM images of the used catalysts.

images show that a segregation of individual nickel particles from the zeolitic support takes place by the formation of the carbon nanotubes following the tip growth mechanism [37]. Metal particle segregation is quite more pronounced for the nanocrystalline zeolite than for the hierarchical ZSM-5 sample. This result indicates that the secondary porosity stabilizes at least partially the Ni particles, hindering their segregation from the zeolitic support as the carbon nanotube growth occurs. Moreover, these findings may explain the differences observed in the behavior of the Ni/ZSM-5 sample along the time on stream compared with the rest of the catalysts as a consequence of the high degree of phase segregation between Ni particles and zeolitic support in this material, once carbon nanotubes have been formed.

The diameter of the nanotubes is controlled by the size of the Ni particles, ranging from 10 to 30 nm. Most of these carbon nanotubes present multiwalled morphology being mainly hollow inside. The existence of several layers on the inner wall of the nanotubes can be appreciated. The space between these layers was estimated around 3.6 Å (measured by counting 10 layers on TEM images), being in agreement with the spacing between graphene layers, approximately 3.4 Å, indicating the graphitic nature of these carbon nanotubes. Graphene layers were not observed on the outer region of nanotubes likely due to their destruction by the high-intense TEM electron beam [38]. It is worth to mention that the catalytic methods reported in the literature for the preparation of carbon nanotubes are based on hydrocarbons cracking. Therefore, despite carbon nanotubes were not the main object of the present work, its formation during the catalytic conversion of rapeseed oil represents a significant added value to the process here investigated.

4. Conclusions

The catalytic conversion of rapeseed oil over nanocrystalline and hierarchical ZSM-5 zeolites shows a high selectivity for the production of light olefins and aromatic hydrocarbons. Within the olefin fraction, ethylene and propene are the most abundant compounds, whereas aromatics consist of benzene, toluene and xylenes. All these hydrocarbons present high interest as raw chemicals. Under the operating conditions selected all the catalysts lead to a total conversion and deoxygenation of rapeseed oil into hydrocarbons. Deoxygenation takes place by decarboxylation, decarbonylation and dehydration pathways.

The use of hierarchical zeolites, having a secondary porosity in addition to the zeolitic micropores, leads to an enhanced production of light olefins at the expense of aromatic hydrocarbons. A reaction scheme has been proposed in which light olefins are formed by successive end-chain cracking reactions of heavier aliphatic hydrocarbons. Oligomerization, cyclization and aromatization reactions of light olefins are proposed to account for the formation of naphthenic and aromatic hydrocarbons. According to this scheme, light olefins are primary cracking products. The shorter diffusion path existing in hierarchical ZSM-5 limits the light olefin conversion through secondary reactions, explaining the observed increase of their concentration in the gaseous stream. A common general trend for all the purely acidic catalysts along the time on stream is observed, consisting on the progressive increase in the amount of aliphatic hydrocarbons at the expense of the rest of the hydrocarbon fractions. These changes are due to the coke deposition over the catalysts, that causes deactivation of the cracking reactions of heavy hydrocarbons.

Incorporation of Ni to the ZSM-5 zeolite catalysts has also significant effects on the product distribution. This metal is well known for its hydrogenation/dehydrogenation properties. Under the conditions employed in this work (relatively high temperature, atmospheric pressure and absence of external source of hydrogen), the role played by the Ni particles is to promote decarboxylation and dehydrogenation reactions. As a result, the concentration of CO_2 and H_2 in the gaseous stream increases sharply. An enhancement is also observed in the light olefins proportion. Likewise, great amount of coke is formed over the Ni-containing catalysts. TEM images of the used catalysts show that this coke is mainly in the form of carbon nanotubes that growth from the Ni nanoparticles. In the case of the nanocrystalline ZSM-5, the Ni particles are located mainly over the external surface of the zeolite crystals, so during the carbon nanotube growth the metal particles are segregated from the zeolitic support. However, for the hierarchical ZSM-5 a great part of the Ni nanoparticles are located within the secondary porosity, being stabilized and therefore, more resistant against segregation during the formation of carbon nanotubes.

In summary, the results obtained in this work show that, by a convenient selection of the operating conditions and the Ni/ZSM-5 catalyst features, it is possible to direct the transformation of rapeseed oil toward the simultaneous production of different valuable chemicals and products, such as hydrogen, light olefins, BTX hydrocarbons and carbon nanotubes.

Acknowledgements

The authors thank the Spanish MICINN for its financial support to the projects ENE2011-29643-C02-01 and ENE2011-29643-C02-02.

References

[1] A. Demirbas, Applied Energy 88 (2011) 3473–3480.
[2] T.L. Chew, S. Bhatia, Bioresource Technology 99 (2008) 7911–7922.
[3] G.W. Huber, A. Corma, Angewandte Chemie International 46 (2007) 7184–7201.
[4] D.Y.C. Leung, X. Wu, M.K.H. Leung, Applied Energy 87 (2010) 1083–1095.
[5] K.D. Maher, D.C. Bressler, Bioresource Technology 98 (2007) 2351–2368.
[6] R. Luque, L. Herrero-Davila, J.M. Campelo, J.H. Clark, J.M. Hidalgo, D. Luna, J.M. Marinas, A.A. Romero, Energy Environmental Science 1 (2008) 542–564.
[7] R. Luque, J.H. Clark, ChemCatChem 3 (2011) 594–597.
[8] N. Taufiqurrahmi, S. Bhatia, Energy Environmental Science 4 (2011) 1087–1112.
[9] Y. Kang Ong, S. Bhatia, Energy 35 (2010) 111–119.
[10] F. Twaiq, N.M. Zabidi, S. Bhatia, Industrial and Engineering Chemistry Research 38 (1999) 3230–3238.
[11] S.P.R. Katikaneni, J.D. Adjaye, N.N. Bakhshi, Canadian Journal of Chemical Engineering 73 (1995) 484–497.
[12] H. Zhang, Y. Cheng, T.P. Vispute, R. Xiao, G.W. Huber, Energy Environmental Science 4 (2011) 2297–2307.
[13] S. van Donk, J.H. Bitter, P. Krijn, De Jong, Applied Catalysis A-General 212 (2001) 97–116.
[14] F. Twaiq, N.M. Zabidi, S. Bhatia, A.R. Mohamed, Fuel Processing Technology 83 (2003) 105–120.
[15] Y.S. Ooi, R. Zakaria, A.R. Mohamed, S. Bhatia, Catalysis Communications 5 (2004) 441–445.
[16] Y.S. Ooi, F. Twaiq, R. Zakaria, A.R. Mohamed, S. Bhatia, Energy Source 25 (2003) 859–869.
[17] Y.S. Ooi, R. Zakaria, A.R. Mohamed, S. Bhatia, Applied Catalysis 274 (2004) 15–23.
[18] N. Taufiqurrahmi, A.R. Mohamed, S. Bhatia, Bioresource Technology 102 (2011) 10686–10694.
[19] N. Taufiqurrahmi, A.R. Mohamed, S. Bhatia, Journal of Chemical Engineering 163 (2010) 413–421.
[20] A.J. Maia, B. Louis, Y.L. Lam, M.M. Pereira, Journal of Catalysis 269 (2010) 103–109.
[21] J.A. Botas, D.P. Serrano, A. García, J. de Vicente, R. Ramos, Catalysis Today 195 (2012) 59–70.
[22] D.P. Serrano, J. Aguado, J.M. Escola, J.M. Rodríguez, A. Peral, Chemistry of Materials 18 (2006) 2462–2464.
[23] J. Jagiello, M. Thommes, Carbon 42 (2004) 1227–1232.
[24] D.P. Serrano, J. Aguado, J.M. Escola, J.M. Rodríguez, Journal of Analytical and Applied Pyrolysis 74 (2005) 353–360.
[25] D.P. Serrano, J. Aguado, J.M. Rodríguez, A. Peral, Journal of Analytical and Applied Pyrolysis 79 (2007) 456–464.
[26] D. Verboekend, R. Caicedo-Realpe, A. Bonilla, M. Santiago, J. Perez-Ramirez, Chemistry of Materials 22 (2010) 4679–4689.
[27] D.P. Serrano, R.A. García, G. Vicente, M. Linares, D. Procházková, J. Čejka, Journal of Catalysis 279 (2011) 366–380.
[28] P.R. Katikaneni, J. Adjaye, R.O. Idem, N.N. Bakhshi, Industrial and Engineering Chemistry Research 35 (1996) 3332–3346.
[29] R.O. Idem, P.R. Katikaneni, N.N. Bakhshi, Fuel Processing Technology 51 (1997) 101–125.
[30] S.M. Sadrameli, A.E.S. Green, W. Seames, Journal of Analytical and Applied Pyrolysis 86 (2009) 1–7.
[31] T.Y. Leng, A.R. Mohamed, S. Bhatia, Canadian Journal of Chemical Engineering 77 (1999) 156–162.
[32] D.P. Serrano, J. Aguado, J.M. Escola, Industrial & Engineering Chemistry Research 39 (2000) 1177–1184.
[33] J.A. Melero, A. García, M. Clavero, Handbook of Biofuels Production: Processes and Technologies, Woodhead Publishing Limited, Cambridge, 2010, pp. 390–419.
[34] A.S. Escobar, F.V. Pinto, H.S. Cerqueira, M.M. Pereira, Applied Catalysis 315 (2006) 68–73.
[35] M. Guisnet, L. Costa, F. Ramoa Ribeiro, Journal of Molecular Catalysis 305 (2009) 69–83.
[36] S. Srihiranpullop, P. Praserthdam, Catalysis Today 93 (2004) 723–727.
[37] J.W. Snoek, G.F. Froment, M. Fowles, Journal of Catalysis 169 (1997) 240–262.
[38] A.G. Nasibulin, A. Moisala, D.P. Brown, E.I. Kauppinen, Carbon 41 (2003) 2711–2724.